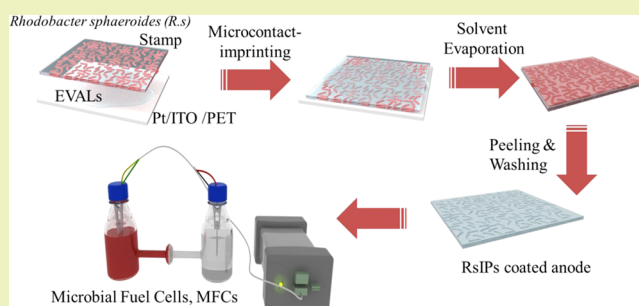


Fabrication of Bacteria-imprinted Polymer Coated Electrodes for Microbial Fuel Cells

Mei-Hwa Lee,[†] James L. Thomas,[‡] Wen-Janq Chen,[§] Ming-Huan Li,[†] Ching-Ping Shih,[§] and Hung-Yin Lin^{*§}[†]Department of Materials Science and Engineering, I-Shou University, Kaohsiung 84001, Taiwan[‡]Department of Physics and Astronomy, University of New Mexico, Albuquerque, New Mexico 87131, United States[§]Department of Chemical and Materials Engineering, National University of Kaohsiung, Kaohsiung 81148, Taiwan

ABSTRACT: The feasibility of using microorganisms for electrical power generation has received considerable interest recently, owing to the environmental concerns regarding fossil fuels and carbon emissions. Bacteria have a high growth rate during cultivation, making them promising for use in microbial fuel cells (MFCs). Using cell-imprinted polymers (CIPs) to enhance microbial binding to the anode is a promising approach; furthermore, elucidating both the synthesis techniques and recognition capabilities of cell-imprinted polymers is also a priority concern in biotechnology. In this work, the anode of a microbial fuel cell was prepared using microcontact imprinting of a cast polymer film. Experimental results indicate that the imprinting polymer solution concentration correlates with the adsorption of bacteria to the finished film. The morphologies of the imprinted cavities, and the distribution of *Rhodobacter sphaeroide* on the *Rhodobacter sphaeroide*-imprinted polymers (RsIPs) was monitored by scanning electron microscopy. Finally, the bacteria-imprinted polymer-coated electrode was used as the anode in a microbial fuel cell to test the performance. The higher output found is likely caused by an increased contact area of bacteria with the anode, increasing electron transfer through a respiratory enzyme.

KEYWORDS: *Rhodobacter sphaeroide*, Microcontact-imprinting, Poly(ethylene-co-vinyl alcohol), Microbial fuel cells



INTRODUCTION

Through a variety of techniques, polymeric films and particles may be imprinted with molecular or cellular templates. Removal of the template then provides a recognition cavity, and rebinding of the template or a similar cell or molecule is enhanced. The mechanisms for cellular recognition are not fully understood; it may involve both molecular recognition and shape recognition. Recent investigations have indicated that shape-selective recognition of an imprinted cavity can enhance the adsorption of microorganisms.^{1,2}

Cell-imprinted polymer (CIP) applications include bioseparation and biosensing of cells through integration with transducers/detectors. Nearly a decade ago, Dickert et al. integrated yeasts,³ viruses⁴ and erythrocytes^{3–7} imprinted polyurethane (PU),^{4–7} on quartz crystal microbalance (QCM) sensing chips. Zare et al. subsequently separated and sorted bacteria by using a polydimethylsiloxane (PDMS) replica.^{8–10} A more recent work used a cell-imprinted substrate on PDMS to control the bone mineralization by MG63 osteoblast-like cells,¹¹ and directed the fate of stem cells.¹² The negative replicas of cell (aka, colloid antibodies)^{1,2} have the silica shell and the deposition of gold nanoparticles on the inner surface to terminate template cells by the photothermal mechanism.¹

Although recognition of small molecules by molecularly imprinted polymers is typically unaffected by the amount of polymer solution concentration used in preparation, for larger targets (e.g., cells), the solution polymer concentration and composition appear to be important, perhaps owing to the larger cavities and the differing recognition mechanisms. We have shown that there is an optimum composition for the imprinted polymers by using microcontact imprinting of algal cells.¹³ Those studies were aimed at coating algal imprinted polymers on the anode for biofuel cells, and showed a higher power output with imprinted polymers than without. This showed that algal imprinted polymers (AIPs) are not only compatible with the living algae but also offer a more conducive environment for the production of electrical energy via the fuel cell.¹⁴

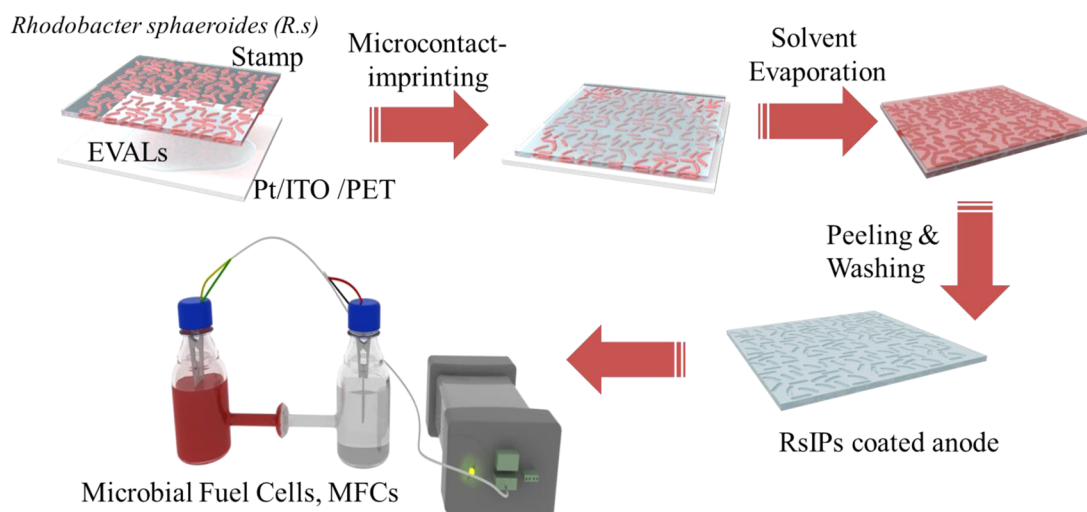
A microbial fuel cell (MFC), a bioreactor, converts chemical energy in organic compounds into electricity.¹⁵ Among the diverse array of MFC applications are electricity generation, bio-hydrogen production, wastewater treatment, biosensors and bioremediation.¹⁵ In addition to providing a testing platform to

Received: February 23, 2015

Revised: April 30, 2015

Published: May 5, 2015

Scheme 1. Preparation of Microcontact *Rhodobacter sphaeroide*-imprinted Pt/ITO/PET Electrode for the Microbial Fuel Cells (MFCs)



characterize anodes, MFCs also offer new opportunities for producing sustainable energy from biodegradable compounds. MFCs have also received considerable attention, owing to their intrinsic advantages¹⁶ in both fundamental studies (especially of anodes) and applications as high throughput platforms (compared to the cultivation and hydrogen production of algae). Recent progress in electrodes for MFCs was reviewed by Wei et al., which discusses how electrode materials, configurations and surface modifications have been developed to improve bacterial adhesion and electron transfer from bacteria to the electrode surface.¹⁷

This work modified the anodic electrodes of MFCs with *Rhodobacter sphaeroide*-imprinted polymers (RsIPs) by using various polymer concentrations to perform microcontact imprinting of bacteria. The readsorption of bacteria to RsIPs was first studied, as well as the surface pore size and imprinting thickness. Finally, the performance of the MFCs was evaluated by using a CIPs-coated electrode as the anode.

MATERIALS AND METHODS

Reagents. *Rhodobacter sphaeroide* (#16407) was purchased from Bioresource Collection and Research Center (BCRC), Hsinchu, Taiwan. Poly(ethylene-co-vinyl alcohol)s (EVALs) containing ethylene of 27, 32, 38 and 44 mol % were purchased from Scientific Polymer Products (Ontario, NY). Dimethyl sulfoxide (DMSO), sodium dodecyl sulfate (SDS), calcium chloride and potassium hydrogen phosphate were from J. T. Baker (ACS grade, NJ). Nafion PFSA Membrane N117 was from DuPont Fuel Cells (Wilmington, DE). Proteose pertone was from Fluka Biochemika (Buchs, Switzerland). Sodium chloride, magnesium sulfate heptahydrate, manganese(II) chloride tetrahydrate, DL-malate and glutamate were from Sigma-Aldrich Co. (St. Louis, MO). Iron(II) sulfate 7-hydrate (99.0%) were also from Panreac (Barcelona, Spain). Sodium molybdate dihydrate was from Alfa Aesar (Ward Hill, MA). Yeast extract was from Becton, Dickinson and Co. (Franklin Lakes, New Jersey). The culture medium for *Rhodobacter sphaeroide* contained 0.2 g/L magnesium sulfate heptahydrate, 1.0 g/L potassium phosphate dibasic, 0.5 g/L sodium chloride, 0.01 g/L, ferrous sulfate monohydrate, 0.02 g/L calcium chloride, 0.002 g/L manganese(II) chloride tetrahydrate, 0.001 g/L sodium molybdate dihydrate, 0.5 g/L yeast extract, 5 g/L DL-malate and 5 g/L glutamate. Trypan Blue solution (0.4%) was from Sigma-Aldrich for the live/dead stain of bacteria. All chemicals were used as received unless otherwise mentioned.

Preparation of Microcontact Imprinting of *Rhodobacter sphaeroide* Thin Films. The preparation of bacteria-imprinted polymer-coated electrodes (as shown in Scheme 1) followed a published protocol¹⁴ with the following changes: An indium tin oxide/poly(ethylene terephthalate) (ITO/PET) thin film (2.5 × 4.2 cm) was cleaned and sputtered with platinum (Pt) at 10 mA for 150 s with an ion sputter coater (Hitachi E-1045). Then glass slides (1.3 × 1.3 cm) were placed in 1.0 mL 1 × 10⁸ cells/mL *Rhodobacter sphaeroide* solutions for 40 min, dried in a hood for another 60 min and used as cellular stamps for cell-imprinting. The EVAL solution (EVAL/DMSO = 5.0–20.0 wt %) was cast onto a bacteria stamp, and the Pt/ITO/PET electrode was placed on the EVAL-coated bacteria stamp and then dried in an oven for 45 min–1 h to evaporate DMSO. Finally, the *Rhodobacter sphaeroide*-imprinted EVAL-coated Pt/ITO/PET electrode was peeled off and washed with deionized water and 0.5 wt % SDS three times, 10 min each time.

Adsorption and Surface Morphology of *Rhodobacter sphaeroide*-imprinted Polymeric Thin Films (RsIPs). The adsorption to the *Rhodobacter sphaeroide*- and nonimprinted polymer films were examined by immersing the films into 1.0 mL of *Rhodobacter sphaeroide* solution (10⁹ cells/mL) for 30 min, and then measuring the *Rhodobacter sphaeroide* concentration in the solution with a UV/vis spectrophotometer (Halo DB-20, Dynamica Pty Ltd., Australia) with absorption wavelength of 800 nm. The *Rhodobacter sphaeroide* concentration can be calibrated with measured optical density. *Rhodobacter sphaeroide*- and nonimprinted polymer films were freeze-dried before examination by a scanning electron microscope (Hitachi S4700, Hitachi High-Technologies Co., Tokyo, Japan). A live/dead stain was performed by adding 10 μL of Trypan Blue and observing with a microscope (CKX41, Olympus, Melville, NY), providing an easy way to visualize living and dead bacteria attached to the electrode.

Performance Measurement of Microbial Fuel Cells (MFCs). All parts were sterilized in an autoclave and irradiated under UV in a laminar flow hood before assembling the fuel cells. The cathode and anode of the biofuel cells contain a platinum wire 5 cm long in 250 mL of PBS, and the *Rhodobacter sphaeroide*-imprinted EVAL-coated Pt/ITO/PET electrode in the culture medium, respectively. A Nafion 117 film (3.0 × 3.0 cm) was used as the proton exchange membrane (PEM). A potentiostat (model 608-1A, CH instruments Inc., Austin, TX) was then employed to measure the maximum voltage (i.e., open circuit voltage, OCV). The polarization and power curves were the plots of current density vs voltage and power output, respectively. Power density ($P = VI/A$) was calculated from the measured current (I) and surface area of the anode electrode (A).¹⁸

RESULTS AND DISCUSSION

Microcontact imprinting is characterized mainly by its high density of imprinted cavities in the imprinted area. In this work, the imprinted stamp preparation and reabsorption concentrations were optimized to yield the highest affinity and capacity between template and imprinted materials or imprinted cavities. Owing to the small size of bacteria (e.g., *Rhodobacter sphaeroide* in this work) compared to algae, the imprinting concentration can be increased to as high as 1.0×10^8 cells/mL to form the adsorption layer of *Rhodobacter sphaeroide* on the glass slide microcontact stamp. A bacteria concentration higher than 1.0×10^9 cells gave a rather high viscosity and was difficult to handle. Then, based on this bacteria concentration, the reabsorption of bacteria was compared with that on nonimprinted material. Figure 1 shows the adsorption of *Rhodobacter sphaeroide* onto

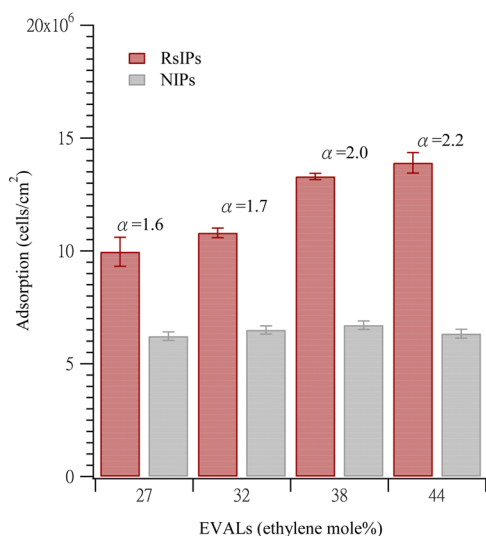


Figure 1. Adsorption of *Rhodobacter sphaeroide* on *Rhodobacter sphaeroide* (Rs)- and nonimprinted EVALs containing different mol % of ethylene. *Rhodobacter sphaeroide* was imprinted and rebound from solution concentrations of 1×10^8 and 1×10^9 cells/mL, respectively, for 30 min.

Rhodobacter sphaeroide-imprinted EVAL thin films, for different mole percentages of ethylene. Imprinting effectiveness (α , the ratio of binding on *Rhodobacter sphaeroide*-imprinted (RsIP) to nonimprinted polymers (NIPs)) was highest ($\alpha = 2.2$) for 44 mol % of ethylene in EVAL, but lowest for the 27 mol %, ($\alpha = 1.6$). In this range, increase in ethylene content increased specific adsorption but not nonspecific adsorption, resulting in increased effectiveness. Adsorption of *Rhodobacter sphaeroide* was always lower than $6.33 \pm 0.20 \times 10^6$ cells/cm² on nonimprinted EVAL thin films and $1.39 \pm 0.45 \times 10^7$ cells/cm² on the imprinted surfaces. Most importantly, for intended applications, the highest total binding of *Rhodobacter sphaeroide* was obtained with 44 mol % ethylene EVAL. This composition was selected for the subsequent microbial fuel cell (MFC) studies.

The imprinting of cells was more easily observed by using scanning electron microscopy (SEM) than by using optical microscopy. Figure 2 shows an SEM image of an RsIPs just peeled from the bacteria stamp. Cavities, some still containing bacteria, are visible, as well as nonimprinted regions. The energy dispersive spectrometer in the microscope allows examination of the surface elements carbon, nitrogen and

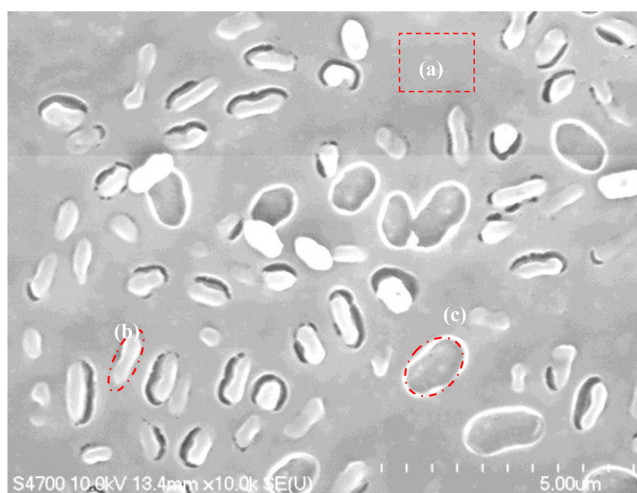


Figure 2. Surface element analysis (carbon, nitrogen and oxygen atomic %) of three locations the *Rhodobacter sphaeroide*-imprinted EVAL (containing 44 mol % of ethylene) thin films (a): NIPs are 66.50, 0.00 and 33.50; (b) *Rhodobacter sphaeroide* on RsIPs are 63.69, 17.25 and 19.06; (c) RsIPs are 86.33, 0.00 and 13.77.

oxygen, reported as an atomic % (ignoring hydrogen.) On three locations of the *Rhodobacter sphaeroide*-imprinted EVAL (containing 44 mol % of ethylene) thin film, the elemental composition was (a), nonimprinted region, 66.50% C, 0.00% N and 33.50% O; (b) a bound *Rhodobacter sphaeroide* bacterium on RsIPs are 63.69% C, 17.25% N and 19.06% O; (c) an apparently vacant recognition cavity 86.33% C, 0.00% N and 13.77% O. The much higher carbon fraction in the recognition cavity may be a result of the imprinting, or may be residue from the bacterial membrane.

The imprinted cells were then removed from RsIPs with surfactants (Figure 3). Figure 3a–d shows the SEM images of RsIPs prepared by using polymer solution concentrations from 5 to 20 wt %. Obviously, partial cells were imprinted at lower polymer concentrations (e.g., 5 and 10 wt %). Notably, a higher concentration of polymer solutions creates a fuller shape of the bacteria-imprinted cavities, i.e., the cavities appear to be deeper and to surround more of each bacterium. Some bacteria were even entrapped in the polymer and could not be removed from RsIPs. Figure 3e shows an SEM image of the bacterial stamp itself; the imprinted cavities in Figure 3a–d thus correspond approximately to the bacterial size. A size analysis of the pores in Figure 3a–d is shown in Figure 3f; the mean pore size was decreased from $0.94 \pm 0.04 \mu\text{m}$ to $0.60 \pm 0.01 \mu\text{m}$ when the polymer concentration increased from 5.0 to 20.0 wt %. Although RsIPs using a higher polymer concentration may form pores with a more complementary structure, the entrapment of bacteria suggests that too high a concentration may reduce the ability to bind new bacteria.

Figure 4 shows the film thickness of RsIPs using different polymer concentrations ranging from 5.0 to 20.0 wt %. The thickness of the RsIPs was increased from $0.93 \pm 0.02 \mu\text{m}$ to $2.56 \pm 0.17 \mu\text{m}$. The average size of *Rhodobacter sphaeroide* shown in Figure 3e is around 2.0–2.5 and 0.5–1.2 μm in length and width, respectively. Therefore, RsIPs prepared using low concentrations (ca. 5.0–10.0 wt %) limits the orientation of bacteria and gives a higher accessible area.

Finally, RsIPs-coated Pt/ITO/PET electrodes were used as the anode of microbial fuel cells (MFCs). Figure 5 shows the time course of the voltage measurements over 70 h and

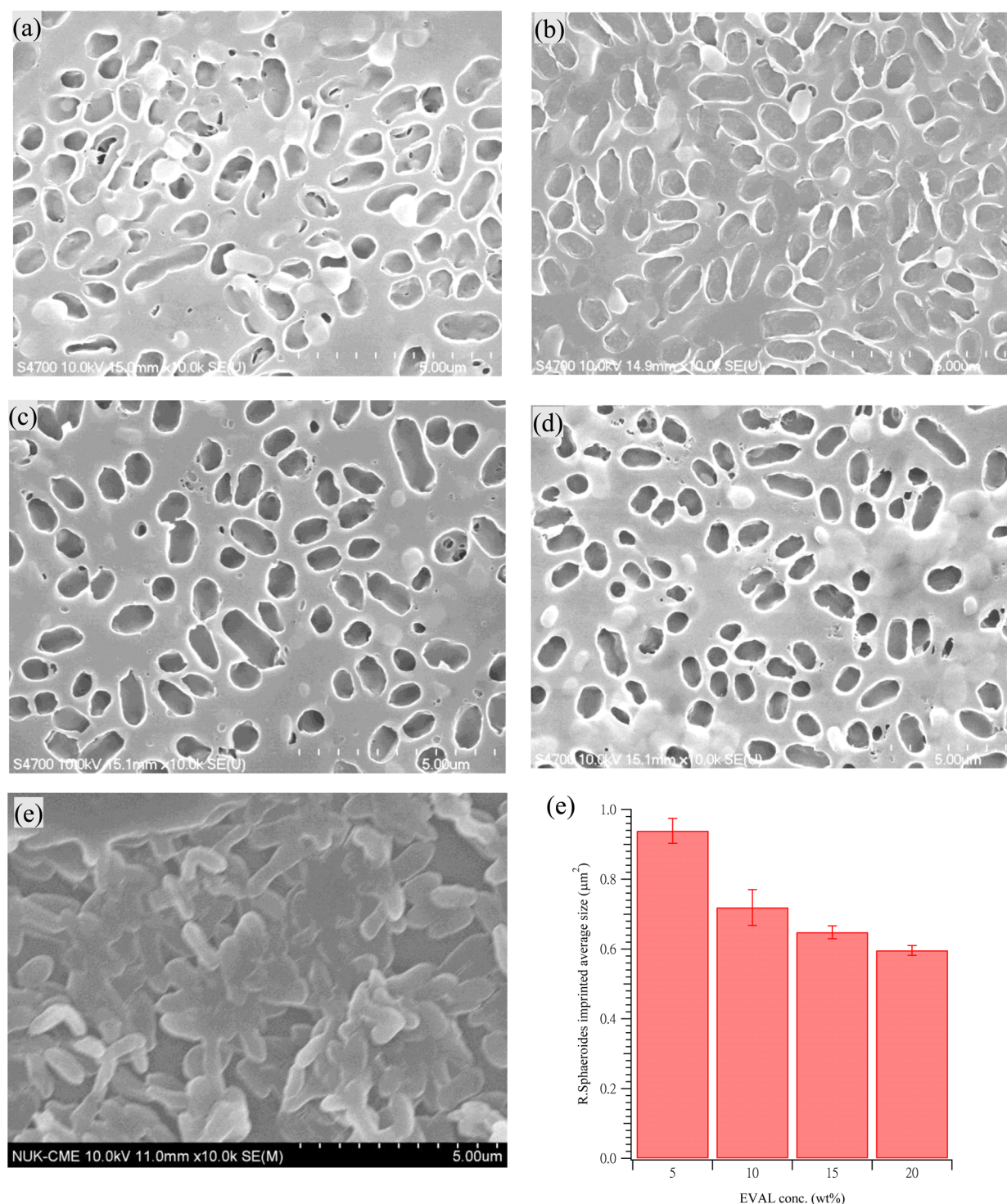


Figure 3. SEM images of the *Rhodobacter sphaeroide*-imprinted EVAL (containing 38 mol % of ethylene) thin films and concentrations of 5.0, 10.0, 15.0 and 20.0 wt % from panels a–d, and (e) the *Rhodobacter sphaeroide* adsorbed stamp. (f) Average imprinted pore size of RsIPs using different EVAL concentrations.

polarization curves loaded with different resistances at 20 h of the MFCs. Compared to the algal fuel cells, the MFCs using RsIPs did not have about 20 h of lag time during the open circuit voltage (OCV) measurements. The OCVs using RsIPs prepared with 5.0 wt % of EVAL (44 ethylene mol %) achieved around 0.48–0.62 V. Microbial fuel cells (MFCs) OCVs using RsIPs, which were prepared using higher polymer concentrations (up to 20 wt %), reduced the stabilized voltage from

0.62 to 0.31 V. Using a bare Pt/ITO/PET electrode as the anode in the MFC yields an even lower OCV at around 0.20 V. The maximum power density using the RsIPs-coated electrode (Figure 5b) also significantly decreased from 1.85 to 0.04 mW/m² when increasing the polymer solution concentration from 5.0 to 20.0 wt %. As shown in this figure, the control experiment using a bare Pt/ITO/PET electrode gave an even lower power density, 0.01 mW/m². Interestingly, the live/dead

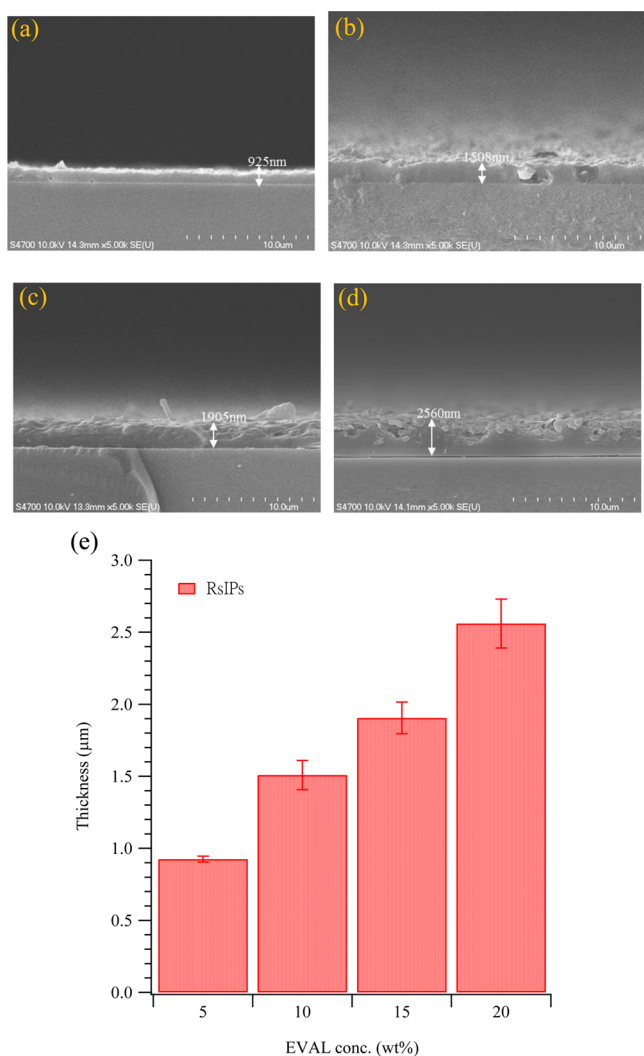


Figure 4. Cross section of RsIPs using 5–20 wt % EVAL concentrations for panels a–d, and (e) the corresponding thicknesses.

stain (Figure 6) demonstrated that the electrode activity is clearly from live cells for the first 20 and 50 h, as most cells excluded the Trypan Blue dye. At 100 h, the higher density of cells makes interpretation less clear, but there are still many living cells.

In MFCs, the bacterial transfer of electrons from the substrates to electrodes is mainly accomplished through two mechanisms: direct transfer (mediator-less) or indirect electron transfer (mediator MFC).¹⁷ In this work, RsIPs likely increase the contact of bacteria with the anode, increasing electron transfer through a respiratory enzyme¹⁹ to enhance the performance in the fuel cell. Moreover, long-range electron transfer¹⁹ may occur through an anode biofilm via conductive pili or an exogenous conductive matrix (for example, carbon nanotube–textile (CNT–textile) composite).²⁰ Multilayer adsorption of bacteria was observed here (Figures 3e and 6), so long-range electron transfer may play a role as well. At any event, the RsIPs seem to provide an initial, stable anchor for the attachment of bacteria to the electrode without losing performance. Certainly, it may be possible to combine RsIP technology with electron-transfer materials or shuttle compounds already demonstrated, to achieve even better performance.

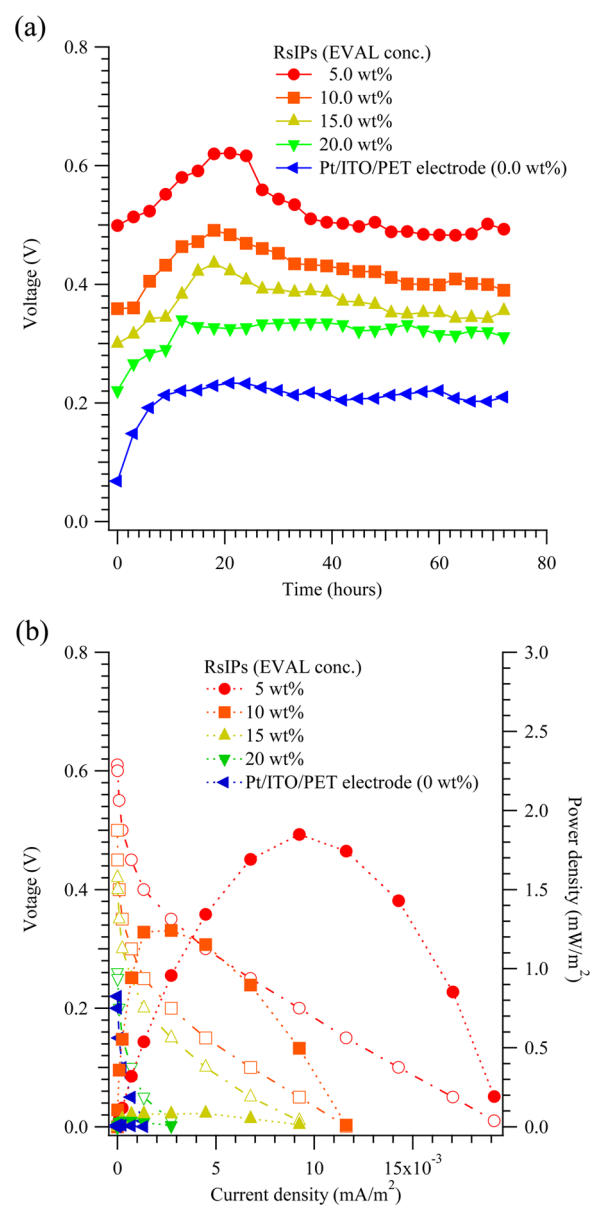


Figure 5. (a) Time course measurements of the open circuit voltage (OCV) of microbial fuel cells using RsIPs-coated and bare Pt/ITO/PET electrodes as the anode. (b) Polarization behavior of the MFCs at 20 h.

CONCLUSIONS

Microbial fuel cells (MFCs) are an effective means of generating electricity from renewable biomass. Cell-imprinted polymer-coated electrodes offer a higher adsorption of bacteria on the electrode surface than blank electrodes, subsequently producing a high power output of MFCs. We have shown that both the composition (ethylene content) and concentration of the polymer solution are important in bacterial recognition and fuel cell performance. Although higher polymer concentration leads to more complete cell imprints, the inability of the RsIP to release the bacteria, or the increased difficulty of electron transport leads to greatly reduced fuel cell performance. The access of bacteria requires a higher open area of imprinted cavities, formed at an optimum polymer concentration. We suggest that the thickness of the cell-imprinted polymer should be no more than half the thickness of the microorganisms in

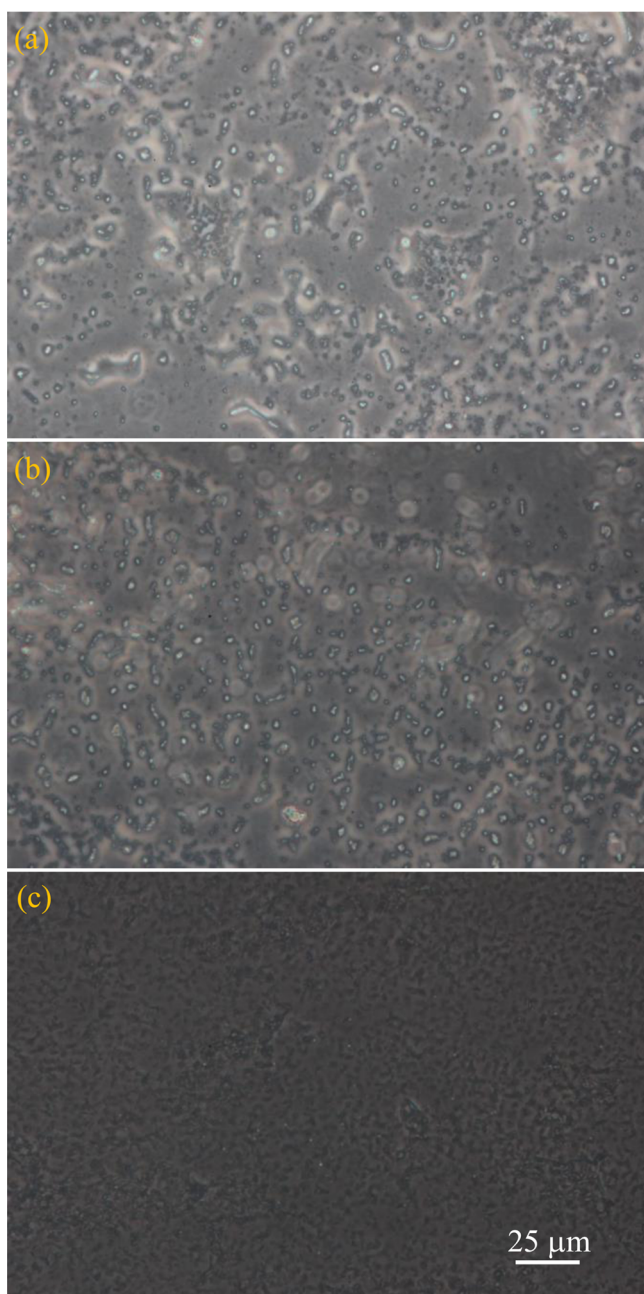


Figure 6. Live/dead staining of bacteria attached to the electrode for (a) 20, (b) 50 and (c) 100 h.

order to achieve the highest adsorption, in keeping with our experimental observations.

AUTHOR INFORMATION

Corresponding Author

*H.-Y. Lin. Address: Department of Chemical and Materials Engineering, National University of Kaohsiung (NUK), 700, Kaohsiung University Rd., Nan-Tzu District, Kaohsiung 811, Taiwan. Tel: (O) +886(7)591-9455; (M) +886(912)178-751. E-mail: linhy@ntu.edu.tw; linhy@caa.columbia.edu.

Notes

The authors declare no competing financial interest.

ACKNOWLEDGMENTS

The authors appreciate the Ministry of Science and Technology of the Republic of China, Taiwan for financially supporting this research under contract nos. MOST 103-2220-E-390-001, 104-2220-E-390-001, 103-2220-E-006-007, 103-2221-E-214-036 and 102-2622-E-214-007 -CC3.

REFERENCES

- (1) Borovička, J.; Metheringham, W. J.; Madden, L. A.; Walton, C. D.; Stoyanov, S. D.; Paunov, V. N. Photothermal colloid antibodies for shape-selective recognition and killing of microorganisms. *J. Am. Chem. Soc.* **2013**, *135*, 5282–5285.
- (2) Borovička, J.; Stoyanov, S. D.; Paunov, V. N. Shape recognition of microbial cells by colloidal cell imprints. *Nanoscale* **2013**, *5*, 8560–8568.
- (3) Dickert, F. L.; Hayden, O. Bioimprinting of polymers and sol–gel phases. Selective detection of yeasts with imprinted polymers. *Anal. Chem.* **2002**, *74*, 1302–1306.
- (4) Jenik, M.; Schirhagl, R.; Schirk, C.; Hayden, O.; Lieberzeit, P.; Blaas, D.; Paul, G.; Dickert, F. L. Sensing picornaviruses using molecular imprinting techniques on a quartz crystal microbalance. *Anal. Chem.* **2009**, *81*, 5320–5326.
- (5) Dickert, F. L.; Hayden, O.; Halikias, K. P. Synthetic receptors as sensor coatings for molecules and living cells. *Analyst* **2001**, *126*, 766–771.
- (6) Hayden, O.; Bindeus, R.; Haderspöck, C.; Mann, K.-J.; Wirl, B.; Dickert, F. L. Mass-sensitive detection of cells, viruses and enzymes with artificial receptors. *Sens. Actuators, B* **2003**, *91*, 316–319.
- (7) Hayden, O.; Lieberzeit, P. A.; Blaas, D.; Dickert, F. L. Artificial antibodies for bioanalyte detection—Sensing viruses and proteins. *Adv. Funct. Mater.* **2006**, *16*, 1269–1278.
- (8) Ren, K.; Zare, R. N. Chemical recognition in cell-imprinted polymers. *ACS Nano* **2012**, *6*, 4314–4318.
- (9) Schirhagl, R.; Hall, E. W.; Fueereder, L.; Zare, R. N. Separation of bacteria with imprinted polymeric films. *Analyst* **2012**, *137*, 1495–1499.
- (10) Ren, K.; Banaei, N.; Zare, R. N. Sorting inactivated cells using cell-imprinted polymer thin films. *ACS Nano* **2013**, *7*, 6031–6036.
- (11) Jeon, H.; Kim, G. Effects of a cell-imprinted poly-(dimethylsiloxane) surface on the cellular activities of MG63 osteoblast-like cells: Preparation of a patterned surface, surface characterization, and bone mineralization. *Langmuir* **2012**, *28*, 13423–13430.
- (12) Mahmoudi, M.; Bonakdar, S.; Shokrgozar, M. A.; Aghaverdi, H.; Hartmann, R.; Pick, A.; Witte, G.; Parak, W. J. Cell-imprinted substrates direct the fate of stem cells. *ACS Nano* **2013**, *7*, 8379–8384.
- (13) Lin, H.-Y.; Hsu, C.-Y.; Thomas, J. L.; Wang, S.-E.; Chen, H.-C.; Chou, T.-C. The microcontact imprinting of proteins: The effect of cross-linking monomers for lysozyme, ribonuclease A and myoglobin. *Biosens. Bioelectron.* **2006**, *22*, 534–543.
- (14) Chen, W.-J.; Lee, M.-H.; Thomas, J. L.; Lu, P.-H.; Li, M.-H.; Lin, H.-Y. Microcontact imprinting of algae on poly(ethylene-co-vinyl alcohol) for biofuel cells. *ACS Appl. Mater. Interfaces* **2013**, *5*, 11123–11128.
- (15) Reddy, V. L.; Kumar, P. S.; Wee, Y.-J. Microbial fuel cells (MFCs) - A novel source of energy for new millennium. In *Current Research, Technology and Education Topics in Applied Microbiology and Microbial Biotechnology*; Méndez-Vilas, A., Ed.; Microbiology Book Series; Formatex Research Center: Spain, 2010; pp 956–964.
- (16) Qian, F.; Morse, D. E. Miniaturizing microbial fuel cells. *Trends Biotechnol.* **2011**, *29*, 62–69.
- (17) Wei, J.; Liang, P.; Huang, X. Recent progress in electrodes for microbial fuel cells. *Bioresour. Technol.* **2011**, *102*, 9335–9344.
- (18) Min, B.; Logan, B. E. Continuous electricity generation from domestic wastewater and organic substrates in a flat plate microbial fuel cell. *Environ. Sci. Technol.* **2004**, *38*, 5809–5814.
- (19) Lovley, D. R. The microbe electric: Conversion of organic matter to electricity. *Curr. Opin. Biotechnol.* **2008**, *19*, 564–571.

(20) Xie, X.; Hu, L.; Pasta, M.; Wells, G. F.; Kong, D.; Criddle, C. S.; Cui, Y. Three-dimensional carbon nanotube–textile anode for high-performance microbial fuel cells. *Nano Lett.* **2011**, *11*, 291–296.